SHIP-1 couples to the Dectin-1 hemITAM and selectively modulates reactive oxygen species production in dendritic cells in response to *C. albicans*

Noelia Blanco-Menéndez[*,‖], Carlos del Fresno[*,‖,#], Sandra Fernandes[†], Enrique Calvo[‡], Ruth Conde-Garrosa[*], William G. Kerr[†,§,¶] and David Sancho[*,#].

[*] *Centro Nacional de Investigaciones Cardiovasculares "Carlos III" (CNIC), Melchor Fernández Almagro 3, Madrid, 28029, Spain.*
[†] *Microbiology and Immunology Department, SUNY Upstate Medical University, Syracuse, New York, USA.*
[‡] *Proteomic Unit, Centro Nacional de Investigaciones Cardiovasculares, CNIC, Madrid, Spain.*
[§] *Pediatrics Department, SUNY Upstate Medical University, Syracuse, New York, USA.*
[¶] *Chemistry Department, Syracuse University, Syracuse, New York, USA.*

[‖] N. B-M and C. del F. contributed equally to this work

[#] Address correspondence to:
David Sancho
Carlos del Fresno
Immunobiology of Inflammation Laboratory
Department of Vascular Biology and Inflammation
Centro Nacional de Investigaciones Cardiovasculares Carlos III (CNIC)
Melchor Fernández Almagro, 3
E-28029, Madrid, Spain
Tel: (+ 34) 914531200 Ext 2010
Tel (direct line): (+ 34) 662 990 4777 2010
FAX: (+ 34) 914531245
E-mail:
dsancho@cnic.es
cdelfresno@cnic.es

Running title: SHIP-1 binds to Dectin-1 to dampen ROS production.

Abstract

Dectin-1 (Clec7a) is a paradigmatic C-type lectin receptor that binds Syk through a hemITAM motif and couples sensing of pathogens such as fungi to induction of innate responses. Dectin-1 engagement triggers a plethora of activating events but little is known about the modulation of such pathways. Trying to define a more precise picture of early Dectin-1 signaling, we explored the interactome of the intracellular tail of the receptor in mouse dendritic cells. We found unexpected binding of SHIP-1 phosphatase to the phosphorylated hemITAM. SHIP-1 co-localized with Dectin-1 during phagocytosis of zymosan in a hemITAM-dependent fashion. Moreover, endogenous SHIP-1 relocated to live or heat-killed *Candida albicans* (HKC)-containing phagosomes in a Dectin-1-dependent fashion in GM-CSF-derived bone marrow cells (GM-BM). However, SHIP-1 absence in GM-BM did not affect activation of MAPK or production of cytokines and readouts dependent on NF-κB and NFAT. Notably, ROS production was enhanced in SHIP-1-deficient GM-BM treated with HKC, live *C. albicans* or the specific Dectin-1 agonists curdlan or whole glucan particles. This increased oxidative burst was dependent on Dectin-1, Syk, PI3K, PDK1 and NADPH oxidase. GM-BM from CD11cΔSHIP-1 mice also showed increased killing activity against live *C. albicans* that was dependent on Dectin-1, Syk and NADPH oxidase. These results illustrate the complexity of myeloid CLR signaling, and how an activating hemITAM can also couple to intracellular inositol phosphatases to modulate selected functional responses and tightly regulate processes such as ROS production that could be deleterious to the host.

Introduction

Aside from their well-known role in the initiation of adaptive immunity, dendritic cells (DC) regulate innate responses that can help clear pathogens. C-type lectin receptors (CLR) expressed on DC are specialized at recognizing the molecular signatures of microbes. Dectin-1 (Clec7a) is a paradigm of signaling CLR expressed on myeloid cells that detects β-1, 3 glucans in a variety of bacteria and fungi (1) and behaves as an activating CLR that promotes inflammation and immunity (2). Upon sensing particulated β-glucans, Dectin-1 is phosphorylated on intracellular tyrosines (3). However, only Y15 phosphorylation in a single YXXL motif termed hemITAM is required for Spleen Tyrosine Kinase (Syk) recruitment and activation (4-8).

Activated Syk mediates recruitment of the CARD9/Bcl10/Malt-1 module that activates the IκB kinase complex for canonical NF-κB signaling (9). Syk phosphorylation also triggers activation of p38, ERK and JNK MAPKs (10), PI3K/Akt (11, 12) and NFAT (13). In addition, some Dectin-1-mediated responses are Syk independent such as the Raf-1 kinase pathway that results in phosphorylation and acetylation of the NF-κB p65 subunit (14), or phagocytosis of zymosan particles in macrophages (15). These signaling events trigger an array of mechanisms that contribute to the elimination of β-glucan-containing pathogens such as *Candida albicans*, including phagocytosis, reactive oxygen species (ROS) production (5), dendritic cell maturation or secretion of cytokines including IL-2, IL-6, IL-10, TNFα and IL-23 (10).

Negative regulation of Syk-mediated activating mechanisms remains relatively undefined and derives mostly from studies on the heterologous regulation by ITIM or inhibitory ITAM-containing receptors (16) that recruit phosphatases such as SH2-containing tyrosine phosphatases (SHP) SHP-1/2 or inositol phosphatases such as

SHIP-1/2 (11, 17). Among CLRs, Clec12a recruits SHP-1 and SHP-2 (18), resulting in the inhibition of Syk-triggered ROS production in response to monosodium urate (19). Notably, Dectin-1 signaling is facilitated by clustering of the receptor in a phagocytic synapse excluding regulatory tyrosine phosphatases CD45 and CD148 (20), but negative modulation of Dectin-1 signaling once the synapse is established is not well defined.

In an attempt to define novel effectors and regulators for Dectin-1 signaling, we have characterized the interactome of the activated Dectin-1 hemITAM by an unbiased proteomic approach. Unexpectedly, we found that SHIP-1 phosphatase associates with Dectin-1 phosphorylated hemITAM. We provide evidence that SHIP-1 has a functional role on Dectin-1 signaling in DC as SHIP-1 relocates along with Dectin-1 to the live or heat-killed *C. albicans* (HKC)-containing phagosome in GM-BM in a Dectin-1-dependent manner. GM-BM from CD11cΔSHIP-1 mice also exhibit augmented ROS production in response to Dectin-1 agonists or *C. albicans*, resulting in increased killing of pathogen. These findings reveal a novel role for SHIP-1 coupling to Dectin-1 hemITAM in the selective control of downstream responses.

Materials and Methods

Reagents and Yeasts

Candida albicans (strain SC5314, kindly provided by Prof. C. Gil, Complutense University, Madrid) was grown on YPD-agar plates (Sigma, St. Louis, MO) at 30°C. HKC was prepared by boiling for 30 minutes. HKC stimulations were performed at a 10:1 ratio except when indicated. Live *C. albicans* was used at a 3:1 ratio except when indicated. When required, HKC was stained with 2.5 mM and live *C. albicans* with 20 μM CFSE or Cell Violet dye (Molecular Probes, Eugene, OR). Curdlan (150 μg/ml, Invivogen, San Diego, CA), WGP (150 μg/ml, Biothera, Eagan, MN), Laminarin (Dectin-1 inhibitor, 200 μg/ml, Sigma), R-406 (Syk inhibitor, 3 μM, Hözel diagnostic, Cologne, Germany), UO126 (Erk inhibitor, 10 μM, Cell Signaling, Danvers, MA), Ly294002 (PI3K inhibitor, 25 μM, Sigma), Bx-795 (PDK1 inhibitor, 1 μM, Abcam, Cambridge, UK), Akt inhibitor VIII (0.75 μM, Calbiochem, Darmstadt, Germany), or DPI (NADPH oxidase inhibitor, 5 μM, Sigma) were used when required. Selected concentrations of inhibitors were chosen after titrating three different doses, and the selected one did not impact cell viability (Data not shown).

Mouse strains and cells

Mouse colonies were bred at CNIC in specific pathogen-free conditions. All animal procedures conformed to EU Directive 2010/63EU and Recommendation 2007/526/EC regarding the protection of animals used for experimental and other scientific purposes, enforced in Spanish law under Real Decreto 1201/2005. CD11c-$^{Cre/+}$ SHIP-1$^{flox/flox}$ (CD11cΔSHIP-1) mice were generated by crossing CD11c$^{Cre/+}$ mice provided by Boris Reizis (Columbia University, New York, USA) (21) with SHIP-1$^{flox/flox}$ mice (22). Frozen bone marrows from *Clec7a*$^{-/-}$ mice (23) and their WT counterparts were kindly

donated by Gordon Brown and Delyth Reid (University of Aberdeen, UK). LysM-$^{Cre/+}$ SHIP-1$^{flox/flox}$ mice were previously described (24). GM-CSF-cultured bone marrow-derived cells (GM-BM) (25) were obtained as described (26) and purified by positive selection using anti-CD11c microbeads (Miltenyi, Bergisch, Germany). SHIP-1 deletion in CD11c^{+} cells was confirmed in purified GM-BM both at the mRNA (Supplemental Fig. 1A) and the protein (Supplemental Fig. 1B) level.

Bone marrow-derived macrophages were obtained after plating total bone marrow cells from WT or LysM-$^{Cre/+}$ SHIP-1$^{flox/flox}$ (LysMΔSHIP-1) mice in culture-treated plates with RPMI 10% FCS supplemented with 20% of L929 supernatant as s source of M-CSF. One day after, 2 millions of non-adherent cells were plated on p60-Petri dishes for 7 days, supplementing with complete fresh medium every 3 days. Macrophages were detached in PBS 5mM EDTA, counted and plated in RPMI 10% FBS. Cells were pre-stimulated for 16 hours with 25 U/ml IFNγ. Cells were exposed to HKC and ROS production was analyzed as indicated.

For neutrophils purification, total bone marrow cells from WT or LysM-$^{Cre/+}$ SHIP-1$^{flox/flox}$ (LysMΔSHIP-1) mice were flushed from tibia and femurs in PBS 2mM EDTA 0.5% FBS. Gradient centrifugation was performed in 65% Percoll (GE Healthcare, Buckinghamshire, UK) for 25 minutes at 4º and 1400 rpms. Pellets were collected and lysed in red blood cells lysis buffer (Sigma). Remaining purified neutrophils (≈ 80% CD11b^{+} Ly6G^{+}) were counted, plated in RPMI 10% FBS and stimulated as indicated.

Pull down and proteomics study

For pull-down assays, C57BL/6 mice were subcutaneously injected with Flt3 ligand-expressing B16 melanoma cells in order to expand the pool of dendritic cells (DC) in the spleen (27). After 12 days, CD11c^{+} cells were isolated and total lysates were

prepared in lysis buffer (TBS - 1% NP40). Soluble lysates or, alternatively, recombinant tSHIP-1 (28) were incubated with biotinylated peptides (GenScript, Piscataway, NJ) corresponding to the cytoplasmic tail of mouse Dectin-1 (NH2-MKYHSHIENLDEDGYTQLDFSTQDIHKR-C, biotin in C-terminal lysine), phosphorylated or not in the Tyr3 and 15, or mouse CD69 (NH2-MDSENCSITENSSSHLERGQKDHGTSIHFEK-C, biotin in C-terminal lysine). Peptides were pulled down using streptavidin-conjugated magnetic beads (Life Technologies, Carlsbad, CA) and interacting proteins were analyzed by mass spectrometry or western blotting using antibodies against SYK (N-1), SHIP-1 (P1C1) for Fig. 1C and Supplemental Fig. 1B or (D20 and V19) for Fig. 1D (Santa Cruz, Dallas, TX), LYN (C13F9) and SHP-2 (#3752) (Cell Signaling). Scaffold software (Proteome software, Runcorn, UK) was used to analyze mass spectrometry data.

Plasmids, constructions, transfection and confocal microscopy

EGFP-tagged SHIP-1 protein was generated by PCR using pExpress vector (Invitrogen) as template and 5'TTTCCCCTCGAGCTATGCCTGCCATGGTCCCTGG-3' and 5'TTTCCCGAATTCGCAGGTCTTCTTCAGAGATCAGTTTCTGTTCGCGGCCGC ACTGCATGGCAGTCCTGCCA-3' as primers. The PCR product was cloned into pEGFP-N1 (Clontech, Mountain View, CA). EGFP-tagged Syk was generated by cloning the coding region for murine Syk, from RAW264.7 cDNA using 5'-CTCGAGACCATGGCGGGAAGTGCTGTGG-3' and 5'-GAATTCGGTTAACCACGTCGTAGTAGT-3' as primers. The PCR product was cloned into pEGFP-N1 (Clontech). For generation of mCherry-tagged wild type Dectin-1 (D-1 WT) or cherry-tagged Dectin-1, where tyrosine 15 was mutated to phenylalanine (D-1 Y15F), we extracted Dectin-1 by PCR using pcDNA.3.1-cloned mouse Dectin-1

as template; WT or Y15F mutated were generated with a mutagenesis kit (Agilent Technologies, Santa Clara, CA) and primers 5'-TTTCCCCTCGAGCCAAATATCACTCTCATATAGA-3' and 5'-TTTCCCGAATTCTTACAGTTCCTTCTCACAGATAC-3' and subsequently cloned into pmCherry-C1 (Clontech).

CHO-K1 cells maintained in complete Ham's F-12 Nutrient Mix supplemented with 10% FBS, 100 U/ml penicillin, 100 μg/ml streptomycin and 2mM L-Glutamine (Gibco, Life technologies) were transiently transfected with the indicated constructions of plasmids using Lipofectamine LTX reagent (Invitrogen, Carlsbad, CA). Transfected cells were grown for 24-48 hours on glass coverslips before the addition of 10 μg/ml of zymosan (Sigma) for 20 min at 37 °C. Cells were then fixed with 0.5% PFA for 30 min, and coverslips were mounted. Confocal images were obtained with a Leica TCSSP5 confocal scanning laser unit attached to an inverted epifluorescence DMI6000B microscope fitted with an HCX PL APO lambda blue 63X/1.4 NA oil immersion objective, using Las-AF acquisition software (Leica, Solms, Germany).

Relocation analysis was performed using ImageJ and IMARIS software (Bitplane, Belfast, UK). Volumes covering the receptor area (red channel) and the total cell area (green channel) were determined. Enrichment index was defined as EI= MGIR/(MGIC-MGIR) where MGIR is the mean green intensity in the receptor volume and MGIC is the mean green intensity in the total cell volume.

Flow cytometry and phagocytosis assay

Phenotypic analysis of GM-BM was performed by flow cytometry using APC-anti-CD11c and FITC-anti-I-A^b (MHC-II) antibodies from eBioscience (Hatfield, UK). Dectin-1 surface expression was assessed by using biotinylated anti-Dectin-1 antibody

(2A11) from Acris (Herford, Germany) and APC-streptavidin from eBioscience. All analysis were pre-gated on live cells determined by Hoechst 33258 incorporation. Dectin-1 expression was assessed inside the $CD11c^+$ gate.

To quantify the phagocytic capacity of Dectin-1 ligands, $CD11c^+$ purified Cell Violet (5 μM)-stained GM-BM were exposed to CFSE-labeled (2.5 μM) HKC for 15 minutes; when indicated, cells were pre-treated for 30 min with laminarin. After extensive washing, cells were recovered on ice with PBS-5mM EDTA. Trypsin-EDTA (0.25%) (Gibco) treatment was used to remove bound, not internalized, HKC particles prior to analysis by flow cytometry. Percentage of engulfed HKC was determined as double positive cells for Cell Violet and CFSE. Internalization of HKC was confirmed by confocal microscopy (Supplemental Fig. 1C).

Immunofluorescence

GM-BM were plated on coverslips and exposed to Cell Violet-stained (2.5 μM) HKC or Cell Violet-stained (20 μM) live *C. albicans* at a 1:3 ratio for 30 minutes. Cells were then fixed with BD Cytofix/Cytoperm (BD Bioscience, San Jose, CA). Phospho-SHIP-1 antibody from Cell Signaling (#3941s) was added and the cells were incubated at 4°C for 24h. Samples were washed and rabbit anti-P-SHIP-1 was detected using the tyramide signal amplification kit (TSA detection kit Alexa Fluor 568, Molecular Probes) as described by the manufacturer. Cells were then mounted with Prolong (Life Technologies) and images were obtained by confocal microscopy. Images were blindly quantified as percentage of P-SHIP-1 positive events among HKCs or live *C. albicans* contacting GM-BM.

Western blot

GM-BM were rested for 4 hours in cell culture medium without FBS and subsequently stimulated at the indicated times with HKC. Cell lysates were prepared in RIPA buffer containing protease and phosphatase inhibitors (Roche, Basel, Switzerland). Samples were run on Mini-PROTEAN TGX PRECAST Gels (BIO-RAD, Hercules, CA) and transferred to a nitrocellulose membrane (BIO-RAD) for blotting with antibodies against β-Actin (C4) from Santa Cruz, P-Syk (C87C1), P-ERK (E10), ERK (#9102s), P-p38 (28B10), p38 (#9212s), P-p40phox (#4311s), IκBα (#9242s), P-Akt (#9275s), Akt (40D4) from Cell Signaling. Alexa Fluor-680 or Qdot-800 conjugated secondary antibodies were used and gels were visualized and quantified in an Odyssey instrument (LI-COR, Lincoln, NE).

Quantitative-PCR

GM-BM were stimulated as indicated and the RNeasy Plus Mini kit (Qiagen) was used for mRNA extraction. cDNA was prepared using the High Capacity cDNA reverse transcription kit (Applied Biosystems, Foster City, CA). Quantitative PCR was performed in a 7900-FAST-384 instrument from Applied Biosystems using the GoTaq qPCR master mix from Promega (Madison, WI). Primers were synthetized by Sigma. Primers used in this work were as follows: SHIP-1 exon-1 Fw: 5'-AGCTGGTAGGAGCAGCAGAG-3'; SHIP-1 exon-1 Rv: 5'-AGTAGCTCCTCTGCCTTGGA– 3'; Egr-3 Fw: 5'-CAACGACATGGGCTCCATTC-3'; Egr-3 Rv: 5'-GGCCTTGATGGTCTCCAGTG– 3'; IL-1β Fw: 5'-TGGTGTGTGACGTTCCCATT-3'; IL-1β Rv: 5'- CAGCACGAGGCTTTTTTGTTG-3'.

Cytokine Determination

Purified GM-BM were left unstimulated or treated overnight with HKC at the indicated ratios. Culture supernatants were collected for cytokine determination by ELISA using kits for TNFα, IL-6, IL-12p40, IL-2 (eBioscience), IL-10 (BD OptEIA) according to the manufacturers´ protocols. Live *C. albicans* was incubated with GM-BM at the indicated ratios for 4 hours and IL-1β was determined in culture supernatants by ELISA (R&D systems, Abingdon, UK).

Measurement of Reactive Oxygen production

Production of reactive oxygen species (ROS) was measured by luminol-enhanced chemiluminescence (20). 100,000 GM-BM were plated in 100 µl of regular culture medium on a 96- well sterile luminometer plate (Corning, Corning, NY). When indicated, GM-BM were pre-treated with different inhibitors for 30 minutes; then, cells were stimulated as indicated and L-012 (Wako Chemicals, Osaka, Japan) was incorporated to the medium (1 mM final concentration) at the beginning of the stimulation. Chemiluminescence was measured at 5 min intervals and expressed as Relative Light Units /second (RLU/s). ROS generation was normalized to maximum PMA-induced (Sigma) ROS production.

Colony forming units counting

GM-BM were plated in 24-well plates and stimulated with live *C. albicans* (1:3 ratio). After 3.5 hours, supernatants were collected and GM-BM were lysed with sterile water to release live yeasts. Supernatants and water were pooled and serial dilutions were prepared and plated on YPD agar plates. In any single experiment, a control condition was run in parallel, where the same amount of live *C. albicans* was grown without GM-

BM. Plates were incubated at 30ºC for 48 hours and colony-forming units (CFUs) were counted. Data are expressed as "% *Candida* killing", resulting from considering the CFUs obtained in the not co-cultured control condition, referred to the CFUs counted in each experimental stimuli.

PAS-hematoxylin staining

GM-BM were coated on coverslips and exposed to live *C. albicans* (1:3 ratio) for 3.5 hours. After fixing with 4% paraformaldehyde for 10 minutes, samples were stained using Periodic Acid Schiff (PAS), counterstained with hematoxylin and examined by light microscopy.

MTT assay

Viability of *C. albicans* after exposure to GM-BM was performed as described (29). In brief, after co-culturing live *C. albicans* and GM-BM (3:1 ratio) for 3.5 hours, medium was removed and a 5 minute incubation was performed with sterile water to lyse GM-BM. Remaining live *C. albicans* were incubated at 37 ºC for 3 hours with 0.5 mg/ml of MTT reagent (Sigma). In any single experiment, a control condition was run in parallel, where the same amount of live *C. albicans* was grown without GM-BM. Subsequently, MTT was removed and newly-formed formazan crystals were dissolved in 0.04 M HCl-isopropanol for 5 minutes at 37 ºC. Absorbance (570 nm) was determined in the resulting solution as a direct measurement of the activity of dehydrogenase on the surface of live *C. albicans*. Data are expressed as "% *Candida* killing", resulting from the formula 100 x 1- ($MTT_{Exp}/MTT_{Control}$), where MTT_{Exp} is the value in the GM-BM and *C. albicans* co-cultures and $MTT_{Control}$ is the value obtained in control wells containing fungus alone.

Statistical analysis

Statistical analysis was performed using Prism software (GraphPad Software, La Jolla, CA). Statistical significance for comparison between two groups of samples coming from a normal distribution (D'Agostino and Pearson omnibus normality test) was determined using the unpaired two-tailed Student's *t* test. For comparison of more than two groups, one-way ANOVA and Bonferroni post-hoc test was used. A p value <0.05 was considered significant (* $p < 0.05$; ** $p< 0.01$; *** $p < 0.001$).

Results

SHIP-1 binds to the phosphorylated hemITAM of Dectin-1.

An unbiased approach to decode the proteome interacting with the intracellular tail of Dectin-1 was designed to screen for novel effectors and regulators of Dectin-1 signaling in DC (Fig. 1A). Lysates from spleen DC were incubated with biotinylated peptides comprising 28 amino acids, corresponding to the intracellular domain of Dectin-1 either unphosphorylated or doubly phosphorylated in Tyr 3 and 15. Controls consisted of the intracellular tail of CD69 or no peptide. Biotin-peptides were pulled down using streptavidin beads and interacting proteins were analyzed by mass spectrometry. A comprehensive list of proteins specific for binding to the Dectin-1 cytoplasmic tail can be found at PeptideAtlas database (www.peptideatlas.org) with the accession number PASS00735. As expected, among the proteins differentially bound to the Tyr-phosphorylated Dectin-1 cytoplasmic tail, Syk kinase was one of the most represented (Fig. 1B, PeptideAtlas #PASS00735) (4). Src kinases, such as Hck and Lyn, or the tyrosine-phosphatase SHP-2, known to interact with Dectin-1 after activation (30, 31), were also detected (Fig. 1B, PeptideAtlas #PASS00735). Unexpectedly, SHIP-1 phosphatase was the Tyr-phosphorylated tail-interacting protein with the highest number of unique peptides recognized (Fig. 1B, PeptideAtlas #PASS00735).

To confirm these findings, we performed Western blot analysis of pulled-down lysates and confirmed specific binding of Syk, Lyn, SHP-2 and SHIP-1 to Dectin-1 Tyr-phosphorylated tail (Fig. 1C). These results suggested that SHIP-1 interacts with the Tyr-phosphorylated Dectin-1 cytoplasmic tail. To examine whether this binding was direct, a recombinant human SHIP-1 variant (tSHIP-1) (28) containing the SH2 domain was assayed with biotinylated Dectin-1 intracellular tail peptides in different conformations: unphosphorylated, distal Tyr (P-Y3)-phosphorylated, proximal Tyr (P-

Y15)-phosphorylated or doubly-phosphorylated (P-Y3,15). Notably, tSHIP-1 was pulled down only by Y15-phosphorylated and doubly phosphorylated Dectin-1 peptides (Fig. 1D). These data indicate that SHIP-1 binds directly the phosphorylated hemITAM in Dectin-1 cytoplasmic tail, and that phosphorylation of Tyr15 is required for SHIP-1 recruitment to Dectin-1.

SHIP-1 co-localizes with Dectin-1 in the phagosome, in a hemITAM-dependent manner.

Upon phagocytosis of specific particulate ligands, Dectin-1 and Syk locate to the phagosome (4, 20). To address whether SHIP-1 colocalizes with Dectin-1 when expressed in cells, we cotransfected CHO cells with wild type (WT) or Y15F Dectin-1-mCherry fusion protein and Syk-EGFP or SHIP-1-EGFP fusion proteins, and evaluated their localization by confocal microscopy upon phagocytosis of zymosan particles. Dectin-1 relocated to the phagosome independently of the Tyr15 of the hemITAM (Fig. 2A, 2B), as reported (6). In contrast, Syk relocation around zymosan-triggered phagosomes was dependent on the presence of Tyr15 (Fig. 2A), as expected (4). Notably, SHIP-1 colocalized with WT but not Y15F Dectin-1 around zymosan phagosomes (Fig. 2B). Analysis of transversal sections across the phagosomes verified the localization (histograms in Fig. 2A, 2B). In summary, both Syk and SHIP-1 fusion proteins similarly colocalized with Dectin-1 WT but not with the Y15F mutant.

To quantify the relocation of Syk or SHIP-1 to the Dectin-1 receptor at the phagosome in an unbiased manner, confocal microscopy images were analyzed by IMARIS software. This enrichment index was defined as Syk-EGFP or SHIP-1-EGFP fluorescence intensity in the Dectin-1-mCherry area (either WT or Y15F) relative to the EGFP intensity in the remainder of the cell. Image analysis revealed a significant

enrichment of Syk and SHIP-1 to the Dectin-1 WT phagosome, but not to the Dectin-1 Y15F phagosome (Fig. 2C). Collectively, these results indicate that, following Dectin-1 activation, both Syk and SHIP-1 are recruited to the intracellular domain of the receptor in a hemITAM-dependent manner, suggesting a potential regulatory role for SHIP-1 in Dectin-1 triggered responses.

SHIP-1 relocates to *C. albicans*-containing phagosomes in GM-BM in a Dectin-1 dependent manner.

To test whether SHIP-1 could have a non-redundant functional effect in Dectin-1 signaling in DC, we generated GM-BM lacking SHIP-1 (Supplemental Fig.1A, 1B) from CD11c$^{Cre/+}$SHIP-1$^{flox/flox}$ (CD11cΔSHIP-1) mice. Our previous analysis of DC compartment in germline SHIP-1$^{-/-}$ mice showed that mature DC are present in normal or increased numbers in spleen and LN, respectively, and that SHIP-1$^{-/-}$ DC possess a normal capacity for priming of antigen-specific T cell responses (32). The *in vitro* differentiation process of WT and CD11cΔSHIP-1 GM-BM cells was similar, as assessed by differentiation markers and numbers of recovered cells from the cultures (Fig. 3A). Notably, Dectin-1 was expressed at the same level in WT and SHIP-1-deleted GM-BM CD11c^{+} cells (Fig. 3B).

We used heat-killed *C. albicans* (HKC) as a model stimulus since the heat-killing process exposes β-glucans (33), resulting in functional responses more dependent on Dectin-1 (34, 35). Following trypsin treatment to remove bound non-internalized HKC (Supplemental Fig. 1C), FACS analysis revealed that Dectin-1-dependent (laminarin-inhibited) uptake of HKC was not affected in CD11cΔSHIP-1 GM-BM compared with WT counterparts (Fig. 3C).

Next, we analyzed SHIP-1 relocation to the *C. albicans*-containing phagosome in primary GM-BM from WT or Dectin-1-deficient mice. SHIP-1 relocated to HKC or live *C. albicans*-containing phagosomes in a Dectin-1 dependent manner (Fig. 3D, 3E). These data support SHIP-1 association to Dectin-1 in GM-BM.

SHIP-1 absence does not affect MAPK activation and cytokine production in response to *C. albicans* in GM-BM.

To investigate a possible role of SHIP-1 in modulation of Dectin-1 signaling, we first analyzed Syk phosphorylation, a critical step for downstream signaling events following detection of HKC by Dectin-1 (36, 37). Stimulation with HKC induced a slight increase in Syk phosphorylation in CD11cΔSHIP-1 compared to WT GM-BM (Fig. 4A). ERK and p38 phosphorylation or IκBα degradation, as a metric of NFκB activation, were comparable between WT and CD11cΔSHIP-1 GM-BM in response to HKC (Fig. 4A). Early growth response (Egr) transcription factors are a family of NFAT-target genes induced in response to Dectin-1 (13). Egr-3 was similarly induced in WT and CD11cΔSHIP-1 GM-BM by HKC (Fig. 4B). Consistent with these results, no differences were observed for TNFα, IL-6, IL-12p40, IL-10 and IL-2 production in response to HKC between WT and CD11cΔSHIP-1 GM-BM (Fig. 4C). IL-1β expression in response to HKC (Fig. 4D) and IL-1β production following stimulation with live *C. albicans* (Fig. 4E), another hallmark of Dectin-1 signaling (38), were also unaffected in the absence of SHIP-1 in GM-BM. These results demonstrate that Dectin-1 engagement in SHIP-1-deficient GM-BM does not lead to significant changes in Syk-mediated signaling pathways and cytokine production.

Enhanced Dectin-1-mediated ROS production in SHIP-1-deficient GM-BM.

Aside from transcriptional activation, Dectin-1-mediated Syk triggering has also been shown to generate ROS (5, 36). To determine the degree of Dectin-1 dependency, we tested HKC-triggered ROS production in GM-BM from WT and *Clec7a*$^{-/-}$ mice (Fig. 5A). The results showed a predominant Dectin-1 dependent, but also a Dectin-1 independent component in ROS induced by HKC in GM-BM. Next, we tested the effect of SHIP-1 absence in HKC-induced ROS. Following exposure to HKC, ROS production was significantly increased in CD11cΔSHIP-1 compared with WT GM-BM, independently of the HKC:GM-BM ratio used (Fig. 5B, Supplemental Fig. 2A). Notably, this effect was specific to CD11c^{+} GM-BM, as the lack of SHIP-1 in M-CSF bone marrow-derived macrophages (Supplemental Fig. 2B) or bone marrow-purified neutrophils (Supplemental Fig. 2C) had no impact on HKC-triggered ROS production.

To test whether the increased ROS production in the absence of SHIP-1 was Dectin-1-dependent, we pretreated GM-BM with laminarin, a soluble β-glucan that inhibits the recognition of specific ligands by Dectin-1 (39) and is capable of impeding *Candida*-induced Dectin-1-mediated ROS production (33). Consistent with Fig. 5A, laminarin pre-treatment inhibited the majority of HKC-induced ROS production and, notably, residual ROS generation was comparable in both WT and CD11cΔSHIP-1 GM-BM (Fig. 5C), supporting that the enhanced HKC-triggered ROS production in SHIP-1-deficient GM-BM was mediated by Dectin-1. Moreover, we tested pure Dectin-1 ligands such as curdlan and whole glucan particles (WGP) (20), which generated ROS in GM-BM in a fully Dectin-1-dependent fashion (Supplemental Fig. 2D, 2E). ROS production was enhanced in SHIP-1 deficient GM-BM in response to curdlan and WGP, a process blocked by laminarin pre-treatment (Fig. 5D, 5E). This set of data illustrated that SHIP-1 regulates ROS production in response to Dectin-1 in GM-BM. Notably, ROS production in response to live *C. albicans* was modest but was also

enhanced in the absence of SHIP-1 in GM-BM (Fig. 5F), suggesting SHIP-1 has a regulatory role on ROS production in response to live fungi.

Syk, PI3K and PDK1 mediate enhanced NADPH oxidase-triggered ROS production in SHIP-1-deficient GM-BM.

To address the signaling pathways leading to increased ROS production in the absence of SHIP-1, we tested ROS production in response to HKC in GM-BM pre-treated with specific inhibitors (5, 36). Consistent with the dependence of ROS production downstream of Dectin-1 on Syk activation (5, 36, 38), the specific Syk inhibitor R-406 fully inhibited ROS generation following HKC sensing (Fig. 6A). Downstream of Dectin-1/Syk, ERK inhibition reduced HKC-triggered ROS production in both WT and CD11cΔSHIP-1 GM-BM (Fig. 6B). Of note, despite an efficient UO126-mediated ERK inhibition (Supplemental Fig. 3A), and a UO126 dose-dependent reduction of IL-1β production in response to live *C. albicans* (Supplemental Fig. 3B), ROS production was still detected in response to HKC. Importantly, the absence of SHIP-1 generated increased ROS levels in the presence of ERK inhibitor (Fig. 6B), suggesting that ERK-dependent ROS were not affected by the regulatory function of SHIP-1.

The phosphatase activity of SHIP-1 antagonizes the kinase activity of PI3K (40). Stimulation with HKC following PI3K inhibition reduced ROS production to the same level in WT and CD11cΔSHIP-1 GM-BM (Fig. 6C), suggesting PI3K as a central mediator of increased ROS production in the absence of SHIP-1. Phosphatidylinositides generated by PI3K recruit Akt (also known as PKB) and phosphoinositide-dependent protein kinase 1 (PDK1) to the membrane (41). Inhibition of Akt kinase (Supplemental Fig. 3C) did not affect HKC-triggered ROS production (Fig. 6D). Notably, inhibition of PDK1 reproduced the results obtained when inhibiting PI3K (Fig. 6E).

Dectin-1-triggered ROS production is mediated by NADPH oxidase (3, 42). Diphenyleneiodonium (DPI), an NADPH oxidase inhibitor (43), abolished HKC-triggered ROS generation in GM-BM (Fig. 6F). Consistent with this observation, direct assessment of the phosphorylation status of the cytosolic p40 subunit of NADPH oxidase revealed increased p40 activation in HKC-treated SHIP-1-deficient but not WT GM-BM (Fig. 6G). Overall, these results show that SHIP-1 non-redundantly regulates ROS production in $CD11c^+$ GM-BM in a Dectin-1/Syk/PI3K/PDK1 and NADPH oxidase-dependent manner.

Enhanced killing activity against *C. albicans* by SHIP-1 deficient GM-BM.

Generation of ROS by myeloid cells is a powerful weapon to fight against *C. albicans* (44, 45). To determine whether the observed increased ROS production in SHIP-1 deficient DC resulted in enhanced candidacidal activity, we co-cultured WT and CD11cΔSHIP-1 GM-BM with live *C. albicans* for 3.5 h and evaluated colony-forming units (CFUs) corresponding to surviving fungus. Following co-culture at a 3:1 *C. albicans*:GM-BM ratio, WT GM-BM exhibited efficient killing activity, indicated as the ratio between live *C. albicans* following the co-culture with GM-BM compared to a control without GM-BM, in which the input *Candida* was unaffected. WT GM-BM *Candida* killing was significantly enhanced in SHIP-1-deficient GM-BM, as gauged by the analysis of remaining CFUs (Fig. 7A). Quantification of live *C. albicans* using the MTT colorimetric assay (29) confirmed the increase in candidacidal activity (Fig. 7B) and visualization of the remaining hyphae by optical microscopy indicated reduced numbers of *C. albicans* following co-culture with SHIP-1 deficient GM-BM (Fig. 7C).

To address whether the increased Dectin-1/Syk/NADPH oxidase-mediated ROS production observed in CD11cΔSHIP-1 GM-BM could account for the enhanced killing

activity, we pretreated cells with laminarin (Fig. 7D), R-406 (Fig. 7E) or DPI (Fig. 7F), and measured killing capacity of GM-BM following coculture. Inhibition of Dectin-1 resulted in a reversal of the improved killing activity in SHIP-1-deficient GM-BM to levels comparable to WT (Fig. 7D). Syk or NADPH oxidase-inhibited GM-BM showed barely detectable candidicidal activity (Fig. 7E, 7F), correlating with fully blocked ROS production (Fig. 6A, 6F). These results support that SHIP-1 non-redundantly modulates a Dectin-1/Syk/NADPH oxidase-mediated pathway regulating candidacidal activity by $CD11c^+$ GM-BM.

Discussion

Dectin-1 is a prototype activating CLR that promotes inflammation and immunity following sensing of β-glucans in the cell wall of fungi and bacteria (1, 2, 5, 10). The hemITAM located in its intracellular domain is primarily considered an activating motif that characterizes a group of myeloid CLRs including Dectin-1, CLEC-2, DNGR-1 and SIGN-R3 (46-49). To explore early effectors and regulators coupling with Dectin-1 hemITAM, we analyzed the interactome of Dectin-1 intracellular tail with DC proteins and found unexpected binding of SHIP-1 phosphatase to the phosphorylated hemITAM. Notably, Dectin-1 guided relocation of SHIP-1 to the zymosan or *Candida*-containing phagosome. At a functional level, SHIP-1 phosphatase selectively antagonize ROS production by a Dectin-1/Syk/PI3K/PDK1/NADPH oxidase-dependent pathway in response to HKC by $CD11c^{+}$ GM-BM.

Our unbiased screen for proteins binding Dectin-1 intracellular tail identified several kinases, including Syk, Hck and Lyn, binding to phosphorylated hemITAM, consistent with previous results (4, 47). Unexpectedly, some intracellular phosphatases also associated with Dectin-1 phosphorylated hemITAM (50), including SHP-2, recently described to associate to Dectin-1 (31). Among these phosphatases, SHIP-1 presented the highest number of unique peptide counts. Interestingly, SHIP-1 has also been found to associate with the CLEC-2 signalosome after receptor activation (51) and to ITAM-domains in activating receptors such as FcγRIIα (52), FcεRIβ (53) or CD79 (54). Since we find that SHIP-1 association to Dectin-1 is dependent on monophosphorylation of the Tyr15 in the hemITAM, the recruitment likely involves the SH2 domain of SHIP-1, similar to the association of SHIP-1 to mono-phosphorylated ITAM (54, 55) or to the association of SHP-2 phosphatase to Dectin-1 (31). Notably, SHIP-1 recruitment to the *Candida*-containing phagosome is dependent on Dectin-1.

In order to determine the relevance of SHIP-1 deletion in DC in response to Dectin-1, we generated $CD11c^+$ GM-CSF-derived bone marrow cells (GM-BM) from CD11cΔSHIP-1 mice where effects of other SHIP-1-deficient cell types on DC function can be excluded (32). We find that, in our culture conditions, CD11cΔSHIP-1 GM-BM differentiated *in vitro* with no significant alterations compared to their WT counterparts in terms of numbers of cells generated or in maturation markers, consistent with our earlier findings of DC maturation and function in lymphoid tissues of germline $SHIP\text{-}1^{-/-}$ mice (32). More recent analysis indicates that myeloid SHIP-1 deficiency, including the DC compartment, does not lead to the myeloproliferative or inflammatory disease that causes the demise of germline $SHIP\text{-}1^{-/-}$ mice (24, 56). Nevertheless, GM-CSF-cultured bone marrow progenitors comprise a heterogeneous population of $CD11c^+$ $MHCII^+$ cells (25), suggesting that different protocols of generation and purification of these cells could impact the obtained results.

Stimulation of CD11cΔSHIP-1 GM-BM with HKC resulted in increased Syk phosphorylation compared with WT GM-BM, although both cells exhibit similar Dectin-1 expression. This result is in accord with previous data indicating an inverse correlation between SHIP-1 expression and Syk phosphorylation (57) and recent findings in human ALL cells showing that inhibition of SHIP-1 induces hyper-phosphorylation of Syk downstream of the B cell receptor (58). Since SHIP-1 is an inositol phosphatase and would not directly affect Syk tyrosine phosphorylation, it is feasible that SHIP-1 and Syk SH2 domains may compete for binding to the phosphorylated Y15 in Dectin-1 hemITAM (59). This competition between SH2 domains for a common phospho-Tyr motifs in receptor tails has been proposed to explain the regulatory role of SHIP-1 at 2B4 in NK cells (60) and TREM-2 in myeloid

cells (61). Moreover, PI3K regulates Syk phosphorylation downstream of the CLEC2 receptor (62), an effect that could be enhanced in the absence of SHIP-1 (40).

Increased phosphorylation of Syk in the absence of SHIP-1 does not result in augmented activation of downstream signaling pathways and transcription factors, including MAPKs, NF-κB or NFAT, thus producing a negligible effect on cytokine production. The only non-redundant effect of SHIP-1 in the modulation of Dectin-1 functional responses is an inhibition of ROS production in response to HKC or live *C. albicans* by $CD11c^+$ GM-BM. This SHIP-1-mediated modulation of Dectin-1 was $CD11c^+$ GM-BM-specific, as it was not found in M-CSF bone marrow-derived macrophages and bone marrow-purified neutrophils deficient in SHIP-1. Divergent data regarding Dectin-1-triggered responses between $CD11c^+$ GM-BM and some other myeloid cells such as bone-marrow derived macrophages or neutrophils have been previously described (63). Similarly, mechanisms involved in *Aspergillus fumigatus*-induced ROS production mediated by PI3K are different between neutrophils and dendritic cells (64).

IL-1β synthesis in response to *C. albicans* depends on ROS production (38). However, despite that SHIP-1-deficient GM-BM showed enhanced ROS generation in response to *C. albicans*, no differences in IL-1β production were detected. On the other hand, ERK was also implicated in IL-1β production (2), but ERK pathway modestly contributes to ROS generation after Dectin-1 ligation (65) and its inhibition does not revert the increased ROS production observed in the absence of SHIP-1. These results suggest that ROS are necessary for IL-1β production but alternative ERK-dependent signals are additionally needed.

We found that SHIP-1-modulated ROS production in response to HKC proceeds *via* the Dectin-1/Syk/PI3K/PDK1/NADPH oxidase axis. PI3K activation has been

implicated in the generation of ROS in response to β-glucan or *Aspergillus fumigatus* (64, 66), although the precise mechanisms linking the Dectin-1/Syk axis with NADPH oxidase activation and ROS production are still a matter of debate. The absence of SHIP-1 or its catalytic activity increases the levels of PIP_3 generated by the Syk-PI3K axis (40, 67) and would explain why PI3K inhibition reverts the increased ROS generation in the absence of SHIP-1. At the same time, PDK1 activity depends on binding to PIP_3 through its PH domain, facilitating not only Akt activation but also some other targets such as p70 ribosomal protein S6 or PKC (68). Although PDK1 does not directly phosphorylate the p40 NADPH subunit (69), the PDK1 target PKC promotes activation of the NADPH oxidase complex (43, 70). Gp91phox and p40phox components of the NADPH oxidase are implicated in Dectin-1-mediated ROS production (71, 72) and in accordance with our results, enhanced ROS production in response to *Saccharomyces cerevisiae* is accompanied by increased p40phox and Syk phosphorylation (42). Thus, SHIP-1 could modulate selectively the balance of effectors in the PI3K pathway activated downstream of Syk after Dectin-1 engagement.

Our results suggest that SHIP-1 regulates the levels of PIP_3 generated by PI3K in response to Dectin-1/Syk stimulation. PIP_3 accumulation in the absence of SHIP-1 would enhance PDK1 activation, NADPH oxidase assembly and ROS production, boosting the killing activity of the cell against Dectin-1 triggering pathogens, such as *C. albicans*. Our data illustrate the complexity of Dectin-1 signaling, where the hitherto considered activating hemITAM can also couple to intracellular phosphatases to selectively regulate certain processes such as ROS production that could be deleterious to the host.

Acknowledgements

We are grateful to Sarai Martínez-Cano, Sudha Neelam, the technicians and assistants at BVI Department, and the Cellomics, Proteomics, Microscopy and Comparative Medicine Units for technical support; to all members of the Immunobiology of Inflammation lab, Vera Rocha and Jose María González-Granado for discussions and critical reading of the manuscript; to Jesús Plá for sharing reagents and discussions; to Kenneth McCreath for editorial assistance; to Gordon Brown and Delyth Reid for providing bone marrows from *Clec7a*$^{-/-}$ mice and their WT counterparts.

Disclosers

The authors declare no conflict of interest.

References

1. Brown, G. D. 2006. Dectin-1: a signalling non-TLR pattern-recognition receptor. *Nat Rev Immunol* 6: 33-43.
2. Drummond, R. A., and G. D. Brown. 2011. The role of Dectin-1 in the host defence against fungal infections. *Current opinion in microbiology* 14: 392-399.
3. Gantner, B. N., R. M. Simmons, S. J. Canavera, S. Akira, and D. M. Underhill. 2003. Collaborative induction of inflammatory responses by dectin-1 and Toll-like receptor 2. *J Exp Med* 197: 1107-1117.
4. Rogers, N. C., E. C. Slack, A. D. Edwards, M. A. Nolte, O. Schulz, E. Schweighoffer, D. L. Williams, S. Gordon, V. L. Tybulewicz, G. D. Brown, and C. Reis e Sousa. 2005. Syk-dependent cytokine induction by Dectin-1 reveals a novel pattern recognition pathway for C type lectins. *Immunity* 22: 507-517.
5. Underhill, D. M., E. Rossnagle, C. A. Lowell, and R. M. Simmons. 2005. Dectin-1 activates Syk tyrosine kinase in a dynamic subset of macrophages for reactive oxygen production. *Blood* 106: 2543-2550.
6. Mansour, M. K., J. M. Tam, N. S. Khan, M. Seward, P. J. Davids, S. Puranam, A. Sokolovska, D. B. Sykes, Z. Dagher, C. Becker, A. Tanne, J. L. Reedy, L. M. Stuart, and J. M. Vyas. 2013. Dectin-1 activation controls maturation of β-1,3-glucan-containing phagosomes. *J Biol Chem* 288: 16043-16054.
7. Robinson, M. J., D. Sancho, E. C. Slack, S. LeibundGut-Landmann, and C. Reis e Sousa. 2006. Myeloid C-type lectins in innate immunity. *Nat Immunol* 7: 1258-1265.
8. Kerrigan, A. M., and G. D. Brown. 2010. Syk-coupled C-type lectin receptors that mediate cellular activation via single tyrosine based activation motifs. *Immunol Rev* 234: 335-352.
9. Gross, O., A. Gewies, K. Finger, M. Schäfer, T. Sparwasser, C. Peschel, I. Förster, and J. Ruland. 2006. Card9 controls a non-TLR signalling pathway for innate anti-fungal immunity. *Nature* 442: 651-656.
10. Leibundgut-Landmann, S., O. Gross, M. Robinson, F. Osorio, E. Slack, S. Tsoni, E. Schweighoffer, V. Tybulewicz, G. Brown, J. Ruland, and C. Reis E Sousa. 2007. Syk- and CARD9-dependent coupling of innate immunity to the induction of T helper cells that produce interleukin 17. *Nat Immunol* 8: 630-638.
11. Lowell, C. A. 2011. Src-family and Syk kinases in activating and inhibitory pathways in innate immune cells: signaling cross talk. *Cold Spring Harb Perspect Biol* 3: 1-16.
12. Cheng, S. C., J. Quintin, R. A. Cramer, K. M. Shepardson, S. Saeed, V. Kumar, E. J. Giamarellos-Bourboulis, J. H. Martens, N. A. Rao, A. Aghajanirefah, G. R. Manjeri, Y. Li, D. C. Ifrim, R. J. Arts, B. M. van der Veer, P. M. Deen, C. Logie, L. A. O'Neill, P. Willems, F. L. van de Veerdonk, J. W. van der Meer, A. Ng, L. A. Joosten, C. Wijmenga, H. G. Stunnenberg, R. J. Xavier, and M. G. Netea. 2014. mTOR- and HIF-1alpha-mediated aerobic glycolysis as metabolic basis for trained immunity. *Science* 345: 1250684.
13. Goodridge, H. S., R. M. Simmons, and D. M. Underhill. 2007. Dectin-1 stimulation by Candida albicans yeast or zymosan triggers NFAT

activation in macrophages and dendritic cells. *J Immunol* 178: 3107-3115.
14. Gringhuis, S. I., J. Den Dunnen, M. Litjens, M. Van Der Vlist, B. Wevers, S. C. M. Bruijns, and T. B. H. Geijtenbeek. 2009. Dectin-1 directs T helper cell differentiation by controlling noncanonical NF-kappaB activation through Raf-1 and Syk. *Nat Immunol* 10: 203-213.
15. Herre, J., A. S. J. Marshall, E. Caron, A. D. Edwards, D. L. Williams, E. Schweighoffer, V. Tybulewicz, C. Reis e Sousa, S. Gordon, and G. D. Brown. 2004. Dectin-1 uses novel mechanisms for yeast phagocytosis in macrophages. *Blood* 104: 4038-4045.
16. Blank, U., P. Launay, M. Benhamou, and R. C. Monteiro. 2009. Inhibitory ITAMs as novel regulators of immunity. *Immunol Rev* 232: 59-71.
17. Redelinghuys, P., and G. D. Brown. 2011. Inhibitory C-type lectin receptors in myeloid cells. *Immunol Lett* 136: 1-12.
18. Marshall, A. S. J., J. A. Willment, H.-H. Lin, D. L. Williams, S. Gordon, and G. D. Brown. 2004. Identification and characterization of a novel human myeloid inhibitory C-type lectin-like receptor (MICL) that is predominantly expressed on granulocytes and monocytes. *J Biol Chem* 279: 14792-14802.
19. Neumann, K., M. Castineiras-Vilarino, U. Hockendorf, N. Hannesschlager, S. Lemeer, D. Kupka, S. Meyermann, M. Lech, H. J. Anders, B. Kuster, D. H. Busch, A. Gewies, R. Naumann, O. Gross, and J. Ruland. 2014. Clec12a is an inhibitory receptor for uric acid crystals that regulates inflammation in response to cell death. *Immunity* 40: 389-399.
20. Goodridge, H. S., C. N. Reyes, C. A. Becker, T. R. Katsumoto, J. Ma, A. J. Wolf, N. Bose, A. S. H. Chan, A. S. Magee, M. E. Danielson, A. Weiss, J. P. Vasilakos, and D. M. Underhill. 2011. Activation of the innate immune receptor Dectin-1 upon formation of a 'phagocytic synapse'. *Nature* 472: 471-475.
21. Caton, M. L., M. R. Smith-Raska, and B. Reizis. 2007. Notch-RBP-J signaling controls the homeostasis of CD8- dendritic cells in the spleen. *J Exp Med* 204: 1653-1664.
22. Wang, J. W., J. M. Howson, T. Ghansah, C. Desponts, J. M. Ninos, S. L. May, K. H. Nguyen, N. Toyama-Sorimachi, and W. G. Kerr. 2002. Influence of SHIP on the NK repertoire and allogeneic bone marrow transplantation. *Science* 295: 2094-2097.
23. Taylor, P. R., S. V. Tsoni, J. A. Willment, K. M. Dennehy, M. Rosas, H. Findon, K. Haynes, C. Steele, M. Botto, S. Gordon, and G. D. Brown. 2007. Dectin-1 is required for beta-glucan recognition and control of fungal infection. *Nat Immunol* 8: 31-38.
24. Park, M. Y., N. Srivastava, R. Sudan, D. R. Viernes, J. D. Chisholm, R. W. Engelman, and W. G. Kerr. 2014. Impaired T-cell survival promotes mucosal inflammatory disease in SHIP1-deficient mice. *Mucosal Immunol* 7: 1429-1439.
25. Helft, J., J. Bottcher, P. Chakravarty, S. Zelenay, J. Huotari, B. U. Schraml, D. Goubau, and E. S. C. Reis. 2015. GM-CSF Mouse Bone Marrow Cultures Comprise a Heterogeneous Population of CD11c(+)MHCII(+) Macrophages and Dendritic Cells. *Immunity* 42: 1197-1211.

26. del Fresno, C., D. Soulat, S. Roth, K. Blazek, I. Udalova, D. Sancho, J. Ruland, and C. Ardavín. 2013. Interferon-beta Production via Dectin-1-Syk-IRF5 Signaling in Dendritic Cells Is Crucial for Immunity to C. albicans. *Immunity* 38: 1176-1186.
27. Mach, N., S. Gillessen, S. B. Wilson, C. Sheehan, M. Mihm, and G. Dranoff. 2000. Differences in dendritic cells stimulated in vivo by tumors engineered to secrete granulocyte-macrophage colony-stimulating factor or Flt3-ligand. *Cancer Res* 60: 3239-3246.
28. Brooks, R., S. Iyer, H. Akada, S. Neelam, C. M. Russo, J. D. Chisholm, and W. G. Kerr. 2015. Coordinate expansion of murine hematopoietic and mesenchymal stem cell compartments by SHIPi. *Stem Cells* 33: 848-858.
29. Levitz, S. M., and R. D. Diamond. 1985. A rapid colorimetric assay of fungal viability with the tetrazolium salt MTT. *J Infect Dis* 152: 938-945.
30. Elsori, D. H., V. P. Yakubenko, T. Roome, P. S. Thiagarajan, A. Bhattacharjee, S. P. Yadav, and M. K. Cathcart. 2011. Protein kinase Cdelta is a critical component of Dectin-1 signaling in primary human monocytes. *J Leukoc Biol* 90: 599-611.
31. Deng, Z., S. Ma, H. Zhou, A. Zang, Y. Fang, T. Li, H. Shi, M. Liu, M. Du, P. R. Taylor, H. H. Zhu, J. Chen, G. Meng, F. Li, C. Chen, Y. Zhang, X. M. Jia, X. Lin, X. Zhang, E. Pearlman, X. Li, G. S. Feng, and H. Xiao. 2015. Tyrosine phosphatase SHP-2 mediates C-type lectin receptor-induced activation of the kinase Syk and anti-fungal TH17 responses. *Nat Immunol* 16: 642-652.
32. Ghansah, T., K. H. T. Paraiso, S. Highfill, C. Desponts, S. May, J. K. McIntosh, J.-W. Wang, J. Ninos, J. Brayer, F. Cheng, E. Sotomayor, and W. G. Kerr. 2004. Expansion of myeloid suppressor cells in SHIP-deficient mice represses allogeneic T cell responses. *J Immunol* 173: 7324-7330.
33. Gantner, B. N., R. M. Simmons, and D. M. Underhill. 2005. Dectin-1 mediates macrophage recognition of Candida albicans yeast but not filaments. *EMBO J* 24: 1277-1286.
34. Netea, M. G., N. A. R. Gow, C. A. Munro, S. Bates, C. Collins, G. Ferwerda, R. P. Hobson, G. Bertram, H. B. Hughes, T. Jansen, L. Jacobs, E. T. Buurman, K. Gijzen, D. L. Williams, R. Torensma, A. McKinnon, D. M. MacCallum, F. C. Odds, J. W. M. Van der Meer, A. J. P. Brown, and B. J. Kullberg. 2006. Immune sensing of Candida albicans requires cooperative recognition of mannans and glucans by lectin and Toll-like receptors. *J Clin Invest* 116: 1642-1650.
35. Gow, N. A., M. G. Netea, C. A. Munro, G. Ferwerda, S. Bates, H. M. Mora-Montes, L. Walker, T. Jansen, L. Jacobs, V. Tsoni, G. D. Brown, F. C. Odds, J. W. Van der Meer, A. J. Brown, and B. J. Kullberg. 2007. Immune recognition of Candida albicans beta-glucan by dectin-1. *J Infect Dis* 196: 1565-1571.
36. Plato, A., J. A. Willment, and G. D. Brown. 2013. C-type lectin-like receptors of the dectin-1 cluster: ligands and signaling pathways. *Int Rev Immunol* 32: 134-156.
37. Sancho, D., and C. Reis e Sousa. 2012. Signaling by Myeloid C-Type Lectin Receptors in Immunity and Homeostasis. *Annu Rev Immunol* 30: 491-529.

38. Gross, O., H. Poeck, M. Bscheider, C. Dostert, N. Hannesschläger, S. Endres, G. Hartmann, A. Tardivel, Schweighoffer, Tybulewicz, A. Mocsai, J. Tschopp, and J. Ruland. 2009. Syk kinase signalling couples to the Nlrp3 inflammasome for anti-fungal host defence. *Nature* 459: 433-436.
39. Brown, G. D., P. R. Taylor, D. M. Reid, J. A. Willment, D. L. Williams, L. Martinez-Pomares, S. Y. C. Wong, and S. Gordon. 2002. Dectin-1 is a major beta-glucan receptor on macrophages. *J Exp Med* 196: 407-412.
40. Kerr, W. G. 2011. Inhibitor and activator: dual functions for SHIP in immunity and cancer. *Ann N Y Acad Sci* 1217: 1-17.
41. Scheid, M. P., and J. R. Woodgett. 2003. Unravelling the activation mechanisms of protein kinase B/Akt. *FEBS Letters* 546: 108-112.
42. Ma, J., C. Becker, C. Reyes, and D. M. Underhill. 2014. Cutting edge: FYCO1 recruitment to dectin-1 phagosomes is accelerated by light chain 3 protein and regulates phagosome maturation and reactive oxygen production. *J Immunol* 192: 1356-1360.
43. Drummond, G. R., S. Selemidis, K. K. Griendling, and C. G. Sobey. 2011. Combating oxidative stress in vascular disease: NADPH oxidases as therapeutic targets. *Nat Rev Drug Discov* 10: 453-471.
44. Donini, M., E. Zenaro, N. Tamassia, and S. Dusi. 2007. NADPH oxidase of human dendritic cells: role in Candida albicans killing and regulation by interferons, dectin-1 and CD206. *Eur J Immunol* 37: 1194-1203.
45. Brothers, K. M., R. L. Gratacap, S. E. Barker, Z. R. Newman, A. Norum, and R. T. Wheeler. 2013. NADPH oxidase-driven phagocyte recruitment controls Candida albicans filamentous growth and prevents mortality. *PLoS Pathogens* 9: e1003634.
46. Fuller, G. L. J., J. A. E. Williams, M. G. Tomlinson, J. A. Eble, S. L. Hanna, S. Pöhlmann, K. Suzuki-Inoue, Y. Ozaki, S. P. Watson, and A. C. Pearce. 2007. The C-type lectin receptors CLEC-2 and Dectin-1, but not DC-SIGN, signal via a novel YXXL-dependent signaling cascade. *J Biol Chem* 282: 12397-12409.
47. Huysamen, C., J. A. Willment, K. M. Dennehy, and G. D. Brown. 2008. CLEC9A is a novel activation C-type lectin-like receptor expressed on BDCA3+ dendritic cells and a subset of monocytes. *J Biol Chem* 283: 16693-16701.
48. Sancho, D., O. P. Joffre, A. M. Keller, N. C. Rogers, D. Martínez, P. Hernanz-Falcón, I. Rosewell, and C. Reis e Sousa. 2009. Identification of a dendritic cell receptor that couples sensing of necrosis to immunity. *Nature* 458: 899-903.
49. Tanne, A., B. Ma, F. Boudou, L. Tailleux, H. Botella, E. Badell, F. Levillain, M. E. Taylor, K. Drickamer, J. Nigou, K. M. Dobos, G. Puzo, D. Vestweber, M. K. Wild, M. Marcinko, P. Sobieszczuk, L. Stewart, D. Lebus, B. Gicquel, and O. Neyrolles. 2009. A murine DC-SIGN homologue contributes to early host defense against Mycobacterium tuberculosis. *J Exp Med* 206: 2205-2220.
50. Iborra, S., and D. Sancho. 2015. Signalling versatility following self and non-self sensing by myeloid C-type lectin receptors. *Immunobiology* 220: 175-184.
51. Parguiña, A. F., J. Alonso, I. Rosa, P. Vélez, M. J. González-López, E. Guitián, J. A. Ebble, M. I. Loza, and A. García. 2012. A detailed proteomic analysis of rhodocytin-activated platelets reveals novel clues

on the CLEC-2 signalosome: implications for CLEC-2 signaling regulation. *Blood* 120: e117-126.
52. Tridandapani, S., Y. Wang, C. B. Marsh, and C. L. Anderson. 2002. Src Homology 2 Domain-Containing Inositol Polyphosphate Phosphatase Regulates NF- B-Mediated Gene Transcription by Phagocytic Fc Rs in Human Myeloid Cells. *J Immunol* 169: 4370-4378.
53. Furumoto, Y., S. Nunomura, T. Terada, J. Rivera, and C. Ra. 2004. The FcepsilonRIbeta immunoreceptor tyrosine-based activation motif exerts inhibitory control on MAPK and IkappaB kinase phosphorylation and mast cell cytokine production. *J Biol Chem* 279: 49177-49187.
54. O'Neill, S. K., A. Getahun, S. B. Gauld, K. T. Merrell, I. Tamir, M. J. Smith, J. M. Dal Porto, Q.-Z. Li, and J. C. Cambier. 2011. Monophosphorylation of CD79a and CD79b ITAM motifs initiates a SHIP-1 phosphatase-mediated inhibitory signaling cascade required for B cell anergy. *Immunity* 35: 746-756.
55. Nakamura, K., A. Malykhin, and K. M. Coggeshall. 2002. The Src homology 2 domain-containing inositol 5-phosphatase negatively regulates Fcgamma receptor-mediated phagocytosis through immunoreceptor tyrosine-based activation motif-bearing phagocytic receptors. *Blood* 100: 3374-3382.
56. Maxwell, M. J., N. Srivastava, M. Y. Park, E. Tsantikos, R. W. Engelman, W. G. Kerr, and M. L. Hibbs. 2014. SHIP-1 deficiency in the myeloid compartment is insufficient to induce myeloid expansion or chronic inflammation. *Genes Immun* 15: 233-240.
57. Roes, J., B. K. Choi, and B. B. Cazac. 2003. Redirection of B cell responsiveness by transforming growth factor beta receptor. *Proc Natl Acad Sci U S A* 100: 7241-7246.
58. Chen, Z., S. Shojaee, M. Buchner, H. Geng, J. W. Lee, L. Klemm, B. Titz, T. G. Graeber, E. Park, Y. X. Tan, A. Satterthwaite, E. Paietta, S. P. Hunger, C. L. Willman, A. Melnick, M. L. Loh, J. U. Jung, J. E. Coligan, S. Bolland, T. W. Mak, A. Limnander, H. Jumaa, M. Reth, A. Weiss, C. A. Lowell, and M. Muschen. 2015. Signalling thresholds and negative B-cell selection in acute lymphoblastic leukaemia. *Nature* 521: 357-361.
59. Conde, C., G. Gloire, and J. Piette. 2011. Enzymatic and non-enzymatic activities of SHIP-1 in signal transduction and cancer. *Biochem Pharmacol* 82: 1320-1334.
60. Wahle, J. A., K. H. Paraiso, R. D. Kendig, H. R. Lawrence, L. Chen, J. Wu, and W. G. Kerr. 2007. Inappropriate recruitment and activity by the Src homology region 2 domain-containing phosphatase 1 (SHP1) is responsible for receptor dominance in the SHIP-deficient NK cell. *J Immunol* 179: 8009-8015.
61. Peng, Q., S. Malhotra, J. A. Torchia, W. G. Kerr, K. M. Coggeshall, and M. B. Humphrey. 2010. TREM2- and DAP12-dependent activation of PI3K requires DAP10 and is inhibited by SHIP1. *Sci Signal* 3: ra38.
62. Manne, B. K., R. Badolia, C. Dangelmaier, J. A. Eble, W. Ellmeier, M. Kahn, and S. P. Kunapuli. 2015. Distinct pathways regulate Syk protein activation downstream of immune tyrosine activation motif (ITAM) and hemITAM receptors in platelets. *J Biol Chem* 290: 11557-11568.

63. Goodridge, H. S., T. Shimada, A. J. Wolf, Y.-M. S. Hsu, C. A. Becker, X. Lin, and D. M. Underhill. 2009. Differential use of CARD9 by Dectin-1 in macrophages and dendritic cells. *J Immunol* 182: 1146-1154.
64. Boyle, K. B., D. Gyori, A. Sindrilaru, K. Scharffetter-Kochanek, P. R. Taylor, A. Mocsai, L. R. Stephens, and P. T. Hawkins. 2011. Class IA phosphoinositide 3-kinase beta and delta regulate neutrophil oxidase activation in response to Aspergillus fumigatus hyphae. *J Immunol* 186: 2978-2989.
65. Li, X. J., C. B. Goodwin, S. C. Nabinger, B. M. Richine, Z. Yang, H. Hanenberg, H. Ohnishi, T. Matozaki, G. S. Feng, and R. J. Chan. 2015. Protein-tyrosine phosphatase Shp2 positively regulates macrophage oxidative burst. *J Biol Chem* 290: 3894-3909.
66. Shah, V. B., T. R. Ozment-Skelton, D. L. Williams, and L. Keshvara. 2009. Vav1 and PI3K are required for phagocytosis of beta-glucan and subsequent superoxide generation by microglia. *Mol Immunol* 46: 1845-1853.
67. Damen, J. E., M. D. Ware, J. Kalesnikoff, M. R. Hughes, and G. Krystal. 2001. SHIP's C-terminus is essential for its hydrolysis of PIP3 and inhibition of mast cell degranulation. *Blood* 97: 1343-1351.
68. Fyffe, C., and M. Falasca. 2013. 3-Phosphoinositide-dependent protein kinase-1 as an emerging target in the management of breast cancer. *Cancer Manag Res* 5: 271-280.
69. Bourdonnay, E., C. H. Serezani, D. M. Aronoff, and M. Peters-Golden. 2012. Regulation of alveolar macrophage p40phox: hierarchy of activating kinases and their inhibition by PGE2. *J Leukoc Biol* 92: 219-231.
70. Raad, H., M. H. Paclet, T. Boussetta, Y. Kroviarski, F. Morel, M. T. Quinn, M. A. Gougerot-Pocidalo, P. M. Dang, and J. El-Benna. 2009. Regulation of the phagocyte NADPH oxidase activity: phosphorylation of gp91phox/NOX2 by protein kinase C enhances its diaphorase activity and binding to Rac2, p67phox, and p47phox. *FASEB J* 23: 1011-1022.
71. Ma, J., C. Becker, C. A. Lowell, and D. M. Underhill. 2012. Dectin-1 triggered recruitment of LC3 to phagosomes facilitates MHC class II presentation of fungal-derived antigens. *J Biol Chem* 287: 34149-34156.
72. Tam, J. M., M. K. Mansour, N. S. Khan, M. Seward, S. Puranam, A. Tanne, A. Sokolovska, C. E. Becker, M. Acharya, M. A. Baird, A. M. Choi, M. W. Davidson, B. H. Segal, A. Lacy-Hulbert, L. M. Stuart, R. J. Xavier, and J. M. Vyas. 2014. Dectin-1-Dependent LC3 Recruitment to Phagosomes Enhances Fungicidal Activity in Macrophages. *J Infect Dis* 219: 1844-1854.

Footnotes

[1] *Non conventional abbreviations:* ROS: Reactive oxygen species; SH2: Src homology 2; SHP: SH2 domain-containing tyrosine phosphatases; Syk: spleen tyrosine kinase

[2] *Grant support:* Work in the DS laboratory is funded by the CNIC and grants from the Spanish Ministry of Economy and Competitiveness (SAF-2013-42920R) and the European Research Council (ERC Starting Independent Researcher Grant 2010, ERC-2010-StG 260414). The CNIC is supported by the Spanish Ministry of Economy and Competitiveness and the Pro-CNIC Foundation. WGK was supported in part by grants from the NIH (R01 HL72523, R01 HL085580, R01 HL107127) and the Paige Arnold Butterfly Run. WGK is the Murphy Family Professor of Children's Oncology Research, an Empire Scholar of the State University of NY and a Senior Scholar of the Crohn's and Colitis Foundation of America.

Figure legends

Figure 1. SHIP-1 binds the phosphorylated hemITAM of Dectin-1.

(**A-C**) Lysates from spleen DC were incubated with peptides representing the intracellular domains of CD69, Dectin-1 or Y3- and Y15- doubly-phosphorylated Dectin-1 (Dectin-1-P). Incubation without peptide was used as a negative control. Pull-down of these peptides was then performed with streptavidin-conjugated beads and interacting proteins were analyzed by mass spectrometry or western blot. **A)** Workflow is shown. **B)** Unique peptide counts determined by mass spectrometry from selected proteins, with their accession numbers. Data indicate unique detected peptides from four independent experiments, with total detected peptides in parenthesis. ND: Not detected. See also PeptideAtlas # PASS00735. **C)** Western blot of selected proteins pulled down in the assay. A representative blot of two performed is shown. **D)** Different concentrations (indicated in nM) of truncated recombinant SHIP-1 (tSHIP-1) were incubated with peptides representing the intracellular domains of non-phosphorylated Dectin-1 (Dectin-1), P-Y3, P-Y15 or P-Y3,15 doubly-phosphorylated Dectin-1. After pull-down, tSHIP-1 was detected by western blot. 100 kDa molecular weight (Mw) marker is shown. tSHIP-1 Mw is 104 kDa. A representative blot of two performed is shown.

Figure 2. SHIP-1 co-localizes with Dectin-1 in the phagosome in a Tyr15-dependent fashion.

(**A-C**) CHO cells expressing either mCherry-tagged wild type Dectin-1 (D-1 WT) or mCherry-tagged Dectin-1 where tyrosine 15 was mutated to phenylalanine (D-1 Y15F), were cotransfected with either EGFP-Syk or EGFP-SHIP-1 fusion proteins. Cells were then exposed to 10 μg/ml of zymosan for 20 minutes and colocalization of Dectin-1 WT or Y15F with Syk (**A**) or SHIP-1 (**B**) was examined by confocal microscopy. Representative images are shown. White lines indicate transversal sections of illustrative phagosomes. Fluorescence intensity profiles for green and red channels are plotted as histograms. Insets show a magnification of the selected region of interest analyzed in the histograms. **C)** Enrichment index of EGFP-tagged

Syk (left panel) and EGFP-tagged SHIP-1 (right panel) in areas where Dectin-1 was detected. Using IMARIS software, the ratio between mean green fluorescence intensity in the receptor area and the rest of the cell was analyzed (See Materials and methods).

Figure 3. SHIP-1 relocates to *Candida albicans* phagosome in GM-BM in a Dectin-1 dependent manner.

GM-BM from wild type (WT) and CD11c$^{Cre/+}$SHIP-1$^{flox/flox}$ (CD11cΔSHIP-1) were generated (**A**) and purified by CD11c-based magnetic bead positive selection (**B,C**). **A**) CD11c and MHC class II expression after 8 days of bone marrow culture with GM-CSF prior to immunomagnetic selection was assessed to evaluate GM-BM differentiation. A representative plot of four independent experiments performed is shown (left panel). Total recovered numbers from these cultures were quantified (right panel). Bars show arithmetic mean + SEM corresponding to eight independent experiments. **B)** Dectin-1 expression was determined by flow cytometry. A representative plot of four independent experiments performed is shown. **C)** Cell Violet-labeled GM-BM were exposed to CFSE-stained HKC at a 1:3 ratio for 15 minutes. When indicated a laminarin pre-treatment was performed for 30 minutes. After extensive washing and trypsin treatment, phagocytosis of the yeasts was analyzed by FACS. Left panels show representative intensity plots. Right histogram depicts arithmetic mean + SEM corresponding to five independent experiments. **D,E)** CD11c^{+} GM-BM from WT or *Clec7a*$^{-/-}$ mice were exposed to Cell Violet-stained heat-killed *Candida albicans* (HKC) (**D**) or Cell Violet-stained live *Candida albicans* (**E**) at a 1:3 ratio for 30 minutes at 37ºC and then fixed, permeabilized, stained for P-SHIP-1 and analyzed by confocal microscopy. White arrows indicate P-SHIP-1 relocation around *Candida*-triggered phagosomes. Right histograms show quantification of P-SHIP-1 events per contacting GM-BM in up to 25 confocal images per genotype. A representative experiment of two is shown.

Figure 4. MAPKs activation and cytokine production in response to *C. albicans* is unaffected in SHIP-1-deficient GM-BM.

(A, B, D) Purified GM-BM from WT and CD11cΔSHIP-1 mice were left unstimulated or treated with HKC (ratio 1:10) for the indicated times. **A)** Syk**,** ERK and p38 MAPK activation and IκBα degradation were analyzed by western blot. A representative blot of four independent experiments is shown. **B)** *Egr-3* mRNA or **D**) *IL-1β* mRNA expression was measured by quantitative PCR. A representative experiment of two performed is shown. **C)** Purified GM-BM from WT and CD11cΔSHIP-1 mice were left unstimulated or treated overnight with HKC at 5:1 or 10:1 HKC:GM-BM ratio. Culture supernatants were collected for TNFα, IL-6, IL-12p40, IL-10 and IL-2 quantification by ELISA. Bars depict arithmetic mean + SEM from three to five independent experiments. **E)** Purified GM-BM from WT and CD11cΔSHIP-1 mice were left unstimulated or treated for 4 hours with live *C. albicans* at 5:1 or 10:1 *C. albicans*:GM-BM ratio. Culture supernatants were collected for IL-1β quantification by ELISA. Bars depict arithmetic mean + SEM from three independent experiments.

Figure 5. Enhanced Dectin-1 -mediated ROS production in SHIP-1-deficient GM-BM.

Purified GM-BM from WT and *Clec7a*$^{-/-}$ (**A**) or from WT and CD11cΔSHIP-1 **(B-F)** mice were left unstimulated or treated with HKC at a 1:10 ratio (**A-C),** 150 μg/ml curdlan **(D)**, 150 μg/ml WGP **(E**) or live *C. albicans* (**F**) at a 1:3 ratio. Dotted line and white bar in **F** denote ROS production by *C. albicans* alone. When indicated, GM-BM were pre-treated for 30 minutes with 200 μg/ml laminarin. Reactive oxygen species (ROS) production was monitored by chemiluminescence during the indicated times and expressed as relative light units per second (RLU/s). Left graphs show a representative experiment. Right histograms show arithmetic mean + SEM of the maximal ROS production corresponding to up to three independent experiments.

Figure 6. Syk, PI3K and PDK1 mediate enhanced NADPH oxidase-triggered ROS production in SHIP-1 deficient GM-BM.

Purified GM-BM from WT and CD11cΔSHIP-1 mice were pretreated for 30 minutes with 3 μM R-406 **(A)**, 10 μM UO126 **(B),** 25 μM Ly294002 **(C),** 0.75 μM Akt inhibitor VIII **(D),** 1 μM BX-795 **(E)** or 5 μM DPI **(F)** prior to stimulation with HKC at a 1:10 ratio. ROS production was monitored by chemiluminescence during the indicated times and expressed as relative light units per second (RLU/s). Left graphs show a representative experiment. Right histograms show arithmetic mean + SEM of the maximal ROS production corresponding to three to four independent experiments. **G**) Purified GM-BM from WT and CD11cΔSHIP-1 mice were exposed to HKC for the indicated times and phospho-p40phox (P-p40phox) was detected by western blot. A representative experiment of three is shown (left panel). Densitometric analysis of P-p40phox relative to β-Actin was conducted (right panel). Bars depict arithmetic mean + SEM from three independent experiments.

Figure 7. SHIP-1 deficient GM-BM exhibit an enhanced killing activity against *C. albicans,* dependent on the Dectin-1/Syk/NADPH oxidase axis.

(A, C) Purified GM-BM (4 x 10^5) from WT and CD11cΔSHIP-1 mice were incubated with live *C. albicans* for 3.5 hours in a *C. albicans*:DC 3:1 ratio. **A)** Supernatants and cell extracts were plated on YPD agar plates and colony forming units (CFUs) were scored to quantify surviving *C. albicans*. Bars depict arithmetic mean + SEM from three independent experiments. **B)** MTT assay to determine remaining live *C. albicans* in supernatant and cell extracts. Histogram shows arithmetic mean + SEM from three independent experiments. **C)** Hyphae formation was visualized by PAS staining, counterstained with hematoxylin. **(D - F)** Purified GM-BM from WT and CD11cΔSHIP-1 mice were pretreated for 30 minutes with 200 μg/ml of laminarin **(D)**, 3 μM R-406 **(E)** or 5 μM DPI **(F)** prior to incubation with live *C. albicans* for 3.5 hours at a 3:1 *C. albicans*:DC ratio. Surviving fungi were quantified by MTT assay as in B). Histograms represent arithmetic mean + SEM from three independent experiments. In all cases, data are

expressed as "% *Candida* killing", resulting from considering the CFUs/MTT values obtained with *C. albicans* alone referred to the CFUs/MTT values measured in each experimental condition.

A

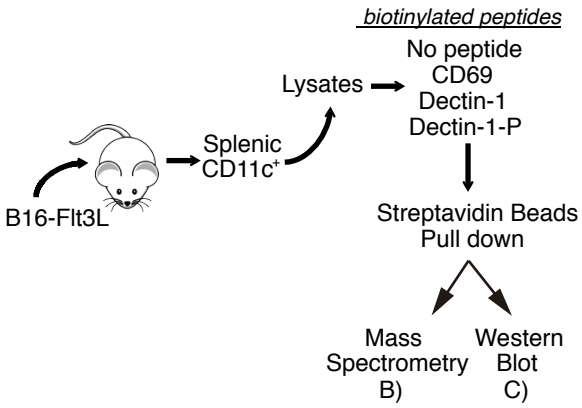

B

Protein name	Accession number	No peptide	CD69	Dectin-1	Dectin-1-P
Kinases					
Syk	gil56550045l	ND	ND	ND	20 (48)
Hck	gil34734056l	ND	ND	ND	8 (10)
Lyn	gil33859588l	ND	ND	ND	3 (3)
Phosphatases					
SHIP-1	gil6754356l	ND	ND	ND	30 (48)
SHP-2	gil6755228l	ND	ND	ND	5 (7)
SHP-1	gil7305133l	ND	ND	ND	3 (3)

C

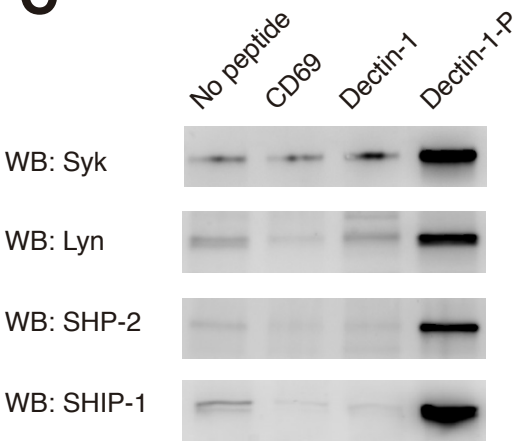

D

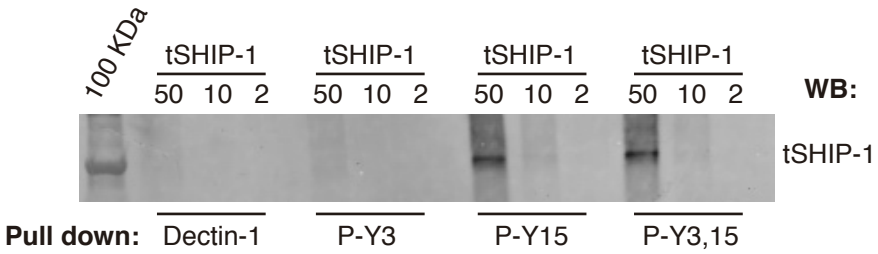

Blanco et al. Figure 1

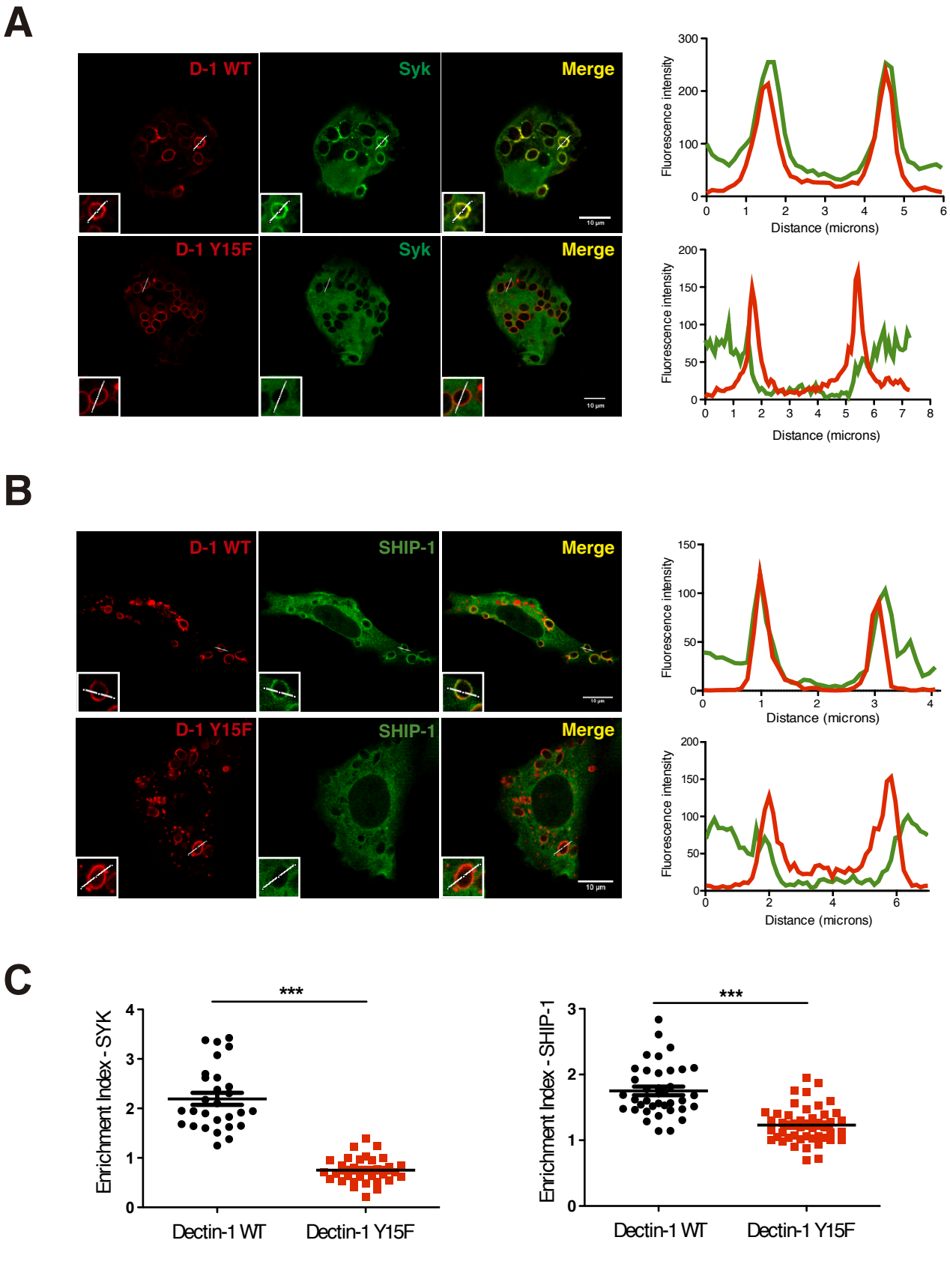

Blanco, et al, Figure 2

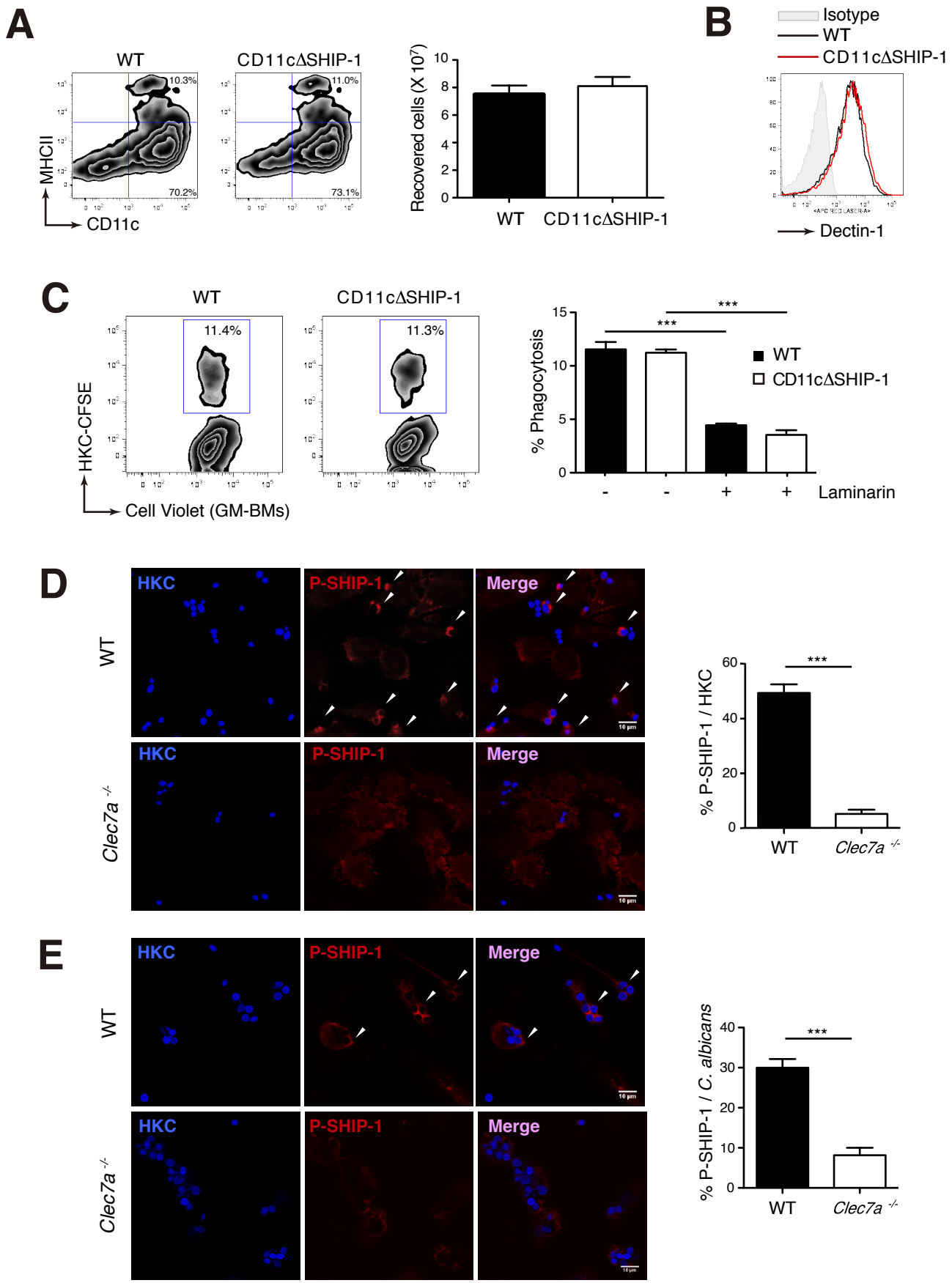

Blanco et al. Figure 3

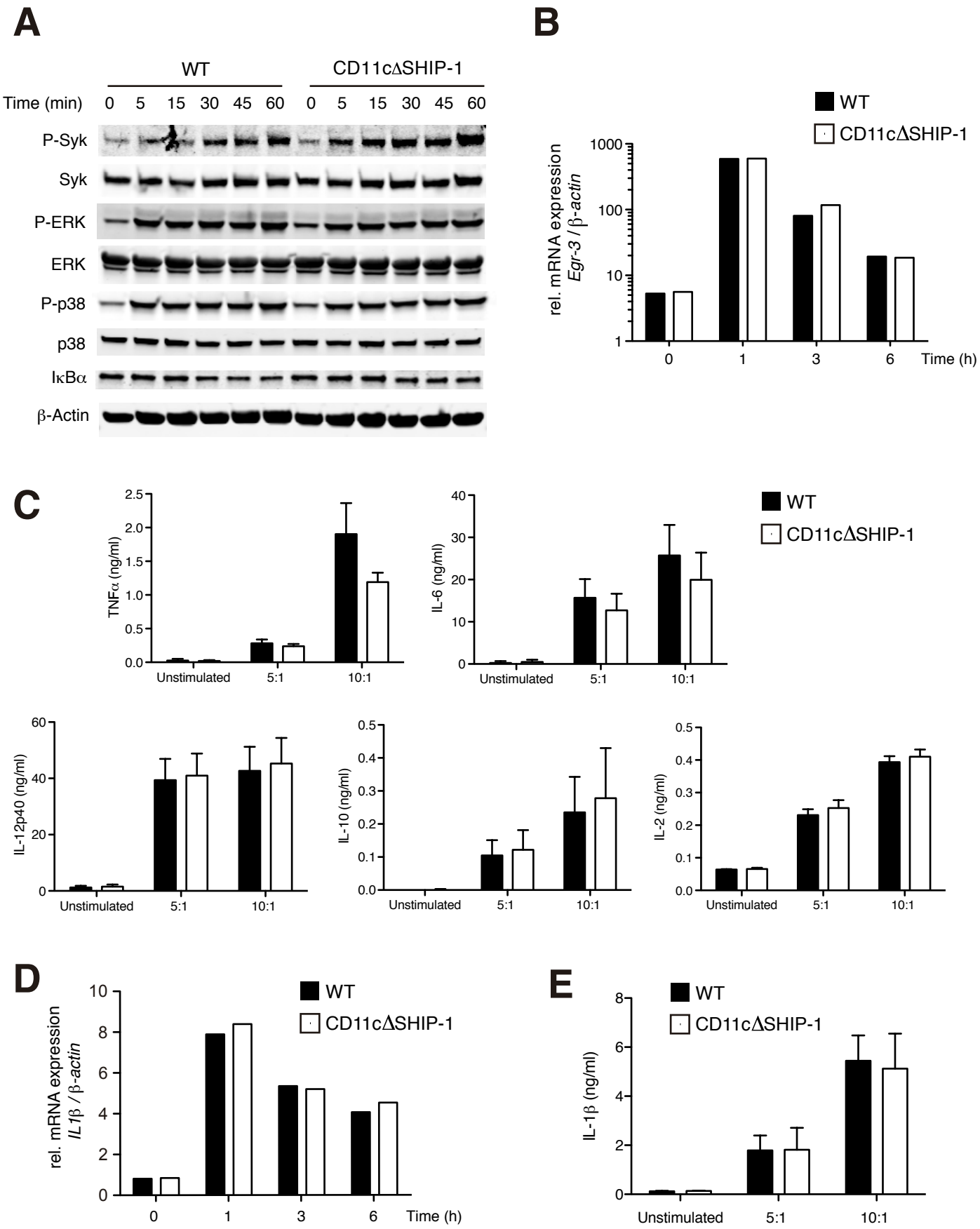

Blanco et al. Figure 4

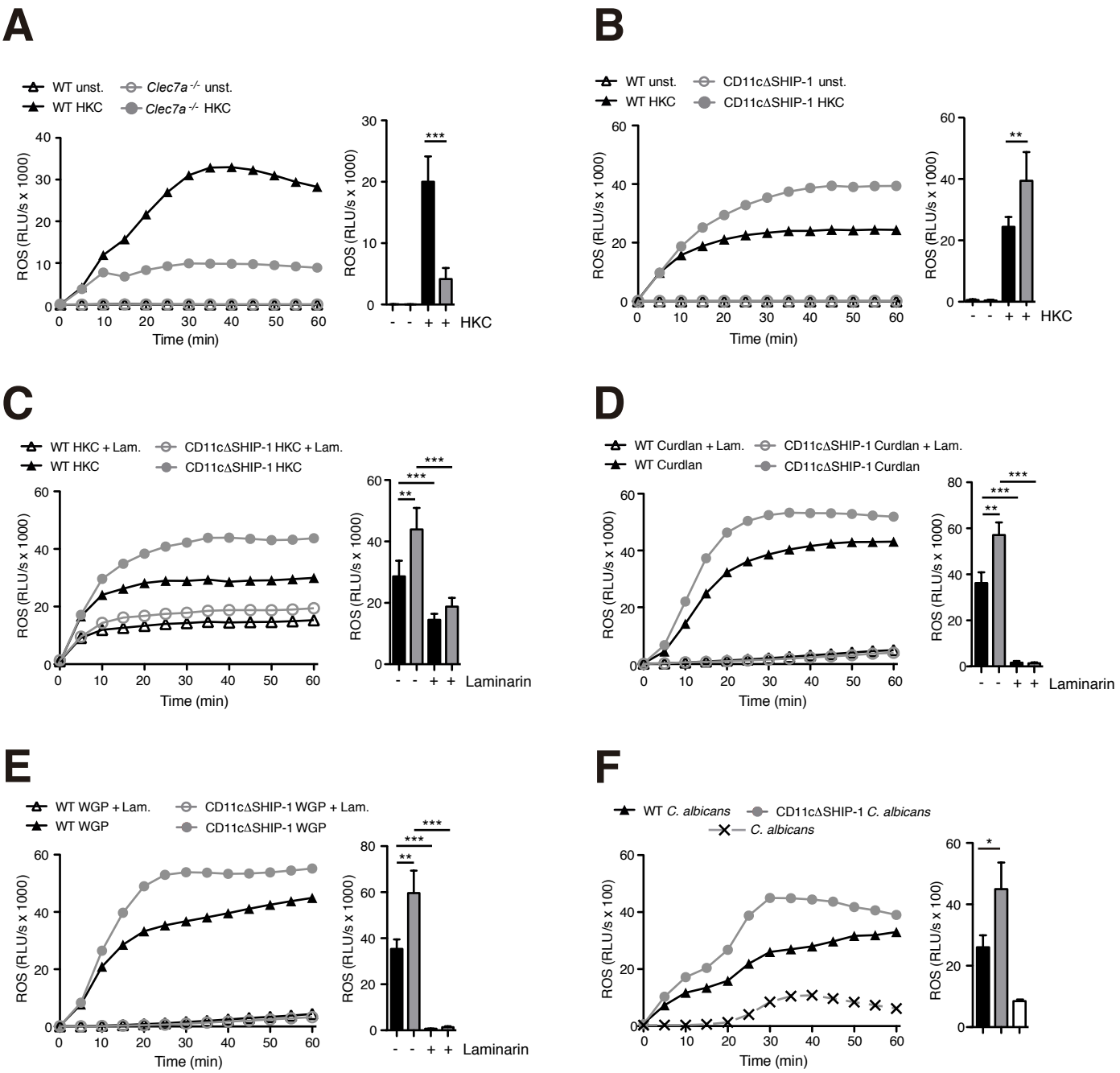

Blanco et al. Figure 5

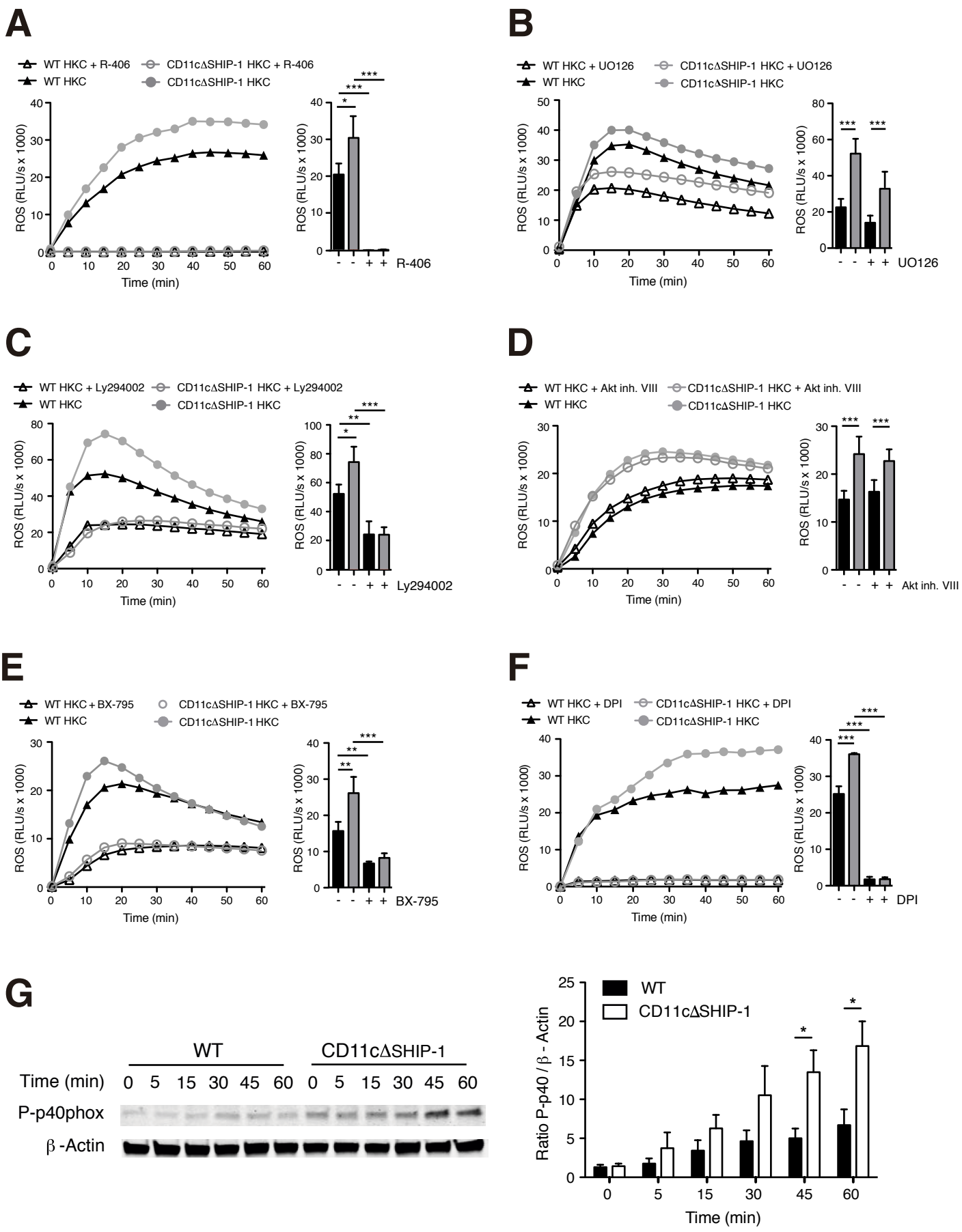

Blanco et al. Figure 6

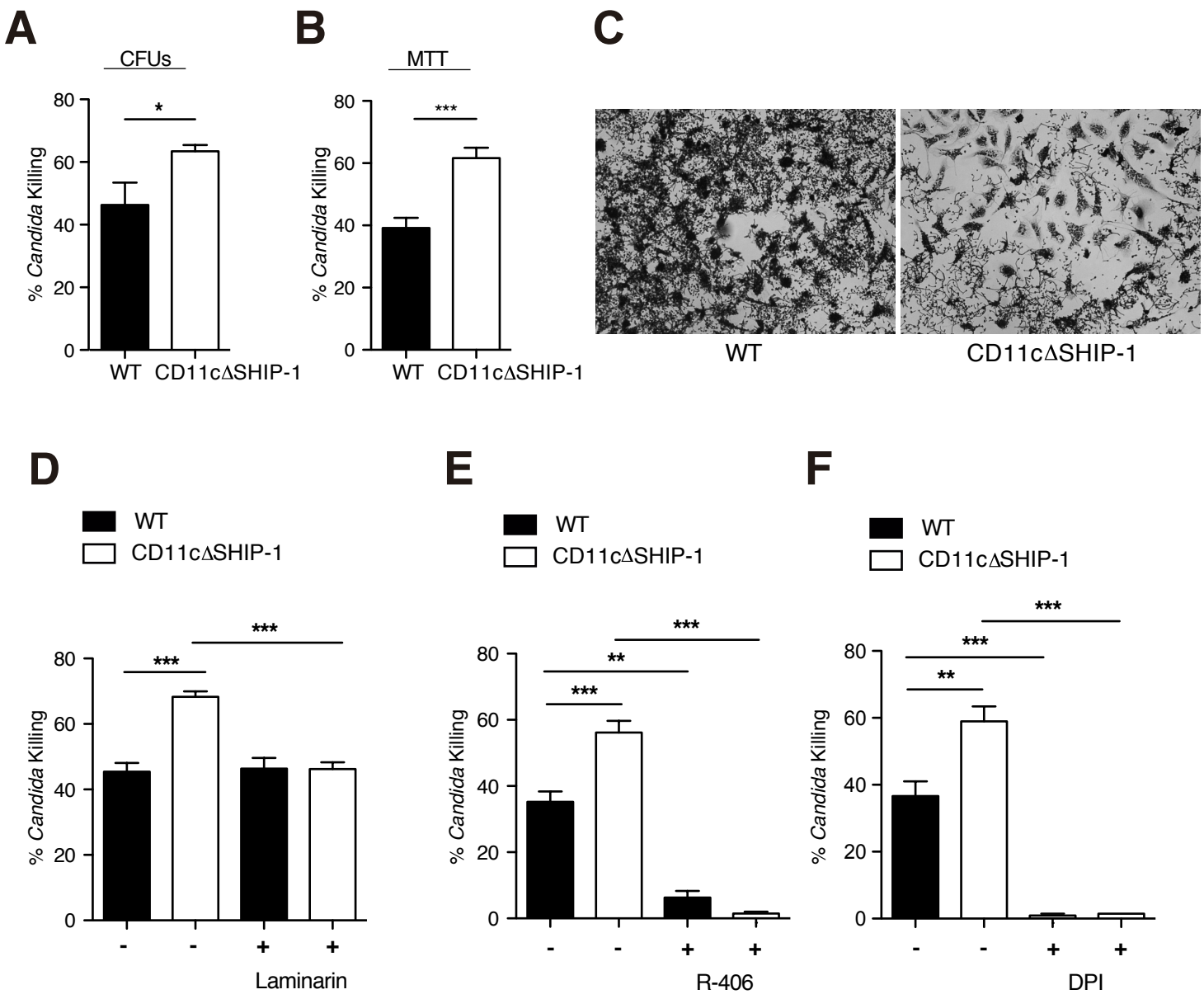

Blanco et al. Figure 7